Reprinted from THE JOURNAL OF THE ACOUSTICAL SOCIETY OF AMERICA, Vol. 42, No. 6, 1278–1286, December 1967

Vibrations of Fluid-Filled Spherical and Spheroidal Shells

R. RAND AND F. DIMAGGIO

Department of Civil Engineering and Engineering Mechanics, Columbia University, New York, New York 10027

Frequency equations and mode shapes are obtained in analytic form for the axisymmetric, extensional, nontorsional vibrations of fluid-filled elastic spherical shells and rigid prolate spheroidal shells, while a numerical scheme is developed for the fluid-filled elastic prolate spheroidal shell. Extensive numerical results in the form of frequency spectra and mode shapes for these problems are displayed.

LIST OF SYMBOLS

a	normal coordinate of shell middle surface, inverse of eccentricity of shell middle surface
a_0, a_1	functions of η; see Eq. B12
$\mathbf{A}$	square matrix; see Eq. 38
b_0, b_1	constants; see Eq. B12
c	velocity of sound progation in fluid
c_s	shear-wave velocity associated with shell material; see Eq. 10
d	interfocal distance; see Figs. 1 and 2
$f_1, f_2, \cdots, f_8$	functions of η defined in Appendix A
F	$R_{0n}^{(1)}$; see Eq. B2
$g_1, g_2, \cdots, g_6$	functions of η defined in Appendix A
G	S_{0n}; see Eq. B3
$h_1, h_2, \cdots, h_6$	functions of η defined in Appendix A
h	minimum shell thickness; see Fig. 2
$J_{n+\frac{1}{2}}$	Bessel function of order $n+\frac{1}{2}$
L_n	Legendre polynomial of degree n
p	dynamic pressure in fluid
P	pressure mode; see Eq. 1
$\mathbf{P}$	column matrix; see Eq. 38
Q	functional defined by Eq. A1
r	radial distance from center of spherical shell
R	radius of spherical shell
$R_{0n}^{(1)}$	prolate spheroidal radial function of the first kind
$s_1, s_2, \cdots, s_5$	functions of η defined in Appendix A
S	auxiliary function defined by Eq. A3
S_{0n}	prolate spheroidal angle function of the first kind
t	time
T	functional defined by Eq. A2
u	tangential displacement of points on shell middle surface; see Fig. 2
U	tangential displacement mode, defined by Eq. 1
w	normal displacement of points on shell middle surface; see Fig. 2
W	normal displacement mode, defined by Eq. 1
z	frequency parameter defined by Eq. 20
$\alpha_1, \alpha_2, \alpha_3$	functions of η defined in Appendix B
$\beta_1, \beta_2, \beta_3, \beta_4$	functions of η defined in Appendix B
γ	frequency parameter defined by Eq. 30
η	tangential ellipsoidal coordinate, see Fig. 1
θ	spherical polar angle
κ	parameter defined by Eq. 8
κ_0	parameter defined by Eq. 22
λ	parameter defined by Eq. 9
λ_{0n}	prolate spheroidal eigenvalue of order 0 and degree n
μ	shear modulus of shell material
ν	Poisson's ratio of shell material
ξ	normal ellipsoidal coordinate; see Fig. 1
ρ	density of fluid
ρ_s	density of shell material
τ	ratio of major to minor axis of shell middle surface; see Eq. 32
ω	natural frequency

INTRODUCTION

EXTENSIONAL axisymmetric vibrations of an elastic spherical shell *in vacuo* were first studied by Lamb.[1] Rayleigh[2] first solved the problem of axisymmetric vibrations of a fluid in a rigid spherical shell. Extensional axisymmetric vibrations of elastic prolate spheroidal shells *in vacuo* were studied by Nemergut and Brand[3] for shells of constant thickness and by DiMaggio and Rand[4] for shells bounded by confocal spheroids. The solution for vibrations of a fluid-filled spherical membrane appears in Morse and Feshbach.[5]

In this paper, frequency equations and mode shapes are obtained in analytic form for the axisymmetric extensional vibrations of fluid-filled elastic spherical shells and rigid prolate spheroidal shells, and a numerical scheme is developed for fluid-filled elastic prolate spheroidal shells. Extensive numerical results in the form of frequency spectra and mode shapes for these problems are displayed.

I. FORMULATION OF THE PROBLEM

Using Flammer's[6] notation, the prolate spheroidal coordinate system and shell geometry are shown in Figs. 1 and 2.

An isotropic elastic shell is bounded by confocal spheroids defined by $\xi=a\pm h/d$, where d is the interfocal distance, h the minimum thickness, and $\xi=a$ (ECCENTRICITY$=1/a$) denotes the middle surface. Extensional, nontorsional shell displacements u and w—respectively, tangent and normal to the shell middle surface—are assumed axisymmetric.

Letting p denote the dynamic pressure of the linear acoustic fluid that fills the shell, and ω a natural frequency, the displacement and pressure modes, U, W, and P, defined by

$$u(\eta,t)=U(\eta)e^{i\omega t},\quad w(\eta,t)=W(\eta)e^{i\omega t},\quad p(\xi,\eta,t)=P(\xi,\eta)e^{i\omega t} \tag{1}$$

satisfy

$$-(1-\eta^2)^{\frac{1}{2}}\frac{d^2}{d\eta^2}[(1-\eta^2)^{\frac{1}{2}}U]-(1-\nu)U-(1-\eta^2)^{\frac{1}{2}}\frac{d}{d\eta}\left\{\left[\frac{\nu}{(a^2-1)^{\frac{1}{2}}}+\frac{(a^2-1)^{\frac{1}{2}}}{a^2-\eta^2}\right]aW\right\}$$
$$-\frac{(1-\nu)\eta(1-\eta^2)^{\frac{1}{2}}}{(a^2-1)^{\frac{1}{2}}(a^2-\eta^2)}aW-\frac{1-\nu}{2}\frac{\rho_s\omega^2d^2}{4\mu}(a^2-\eta^2)U=0, \tag{2}$$

$$\left[\frac{\nu}{(a^2-1)^{\frac{1}{2}}}+\frac{(a^2-1)^{\frac{1}{2}}}{a^2-\eta^2}\right]\frac{d}{d\eta}[(1-\eta^2)^{\frac{1}{2}}aU]-\frac{(1-\nu)\eta(1-\eta^2)^{\frac{1}{2}}}{(a^2-1)^{\frac{1}{2}}(a^2-\eta^2)}aU+\left[\frac{1}{a^2-1}+\frac{2\nu}{a^2-\eta^2}+\frac{a^2-1}{(a^2-\eta^2)^2}\right]a^2W$$
$$-\frac{1-\nu}{2}\frac{\rho_s\omega^2d^2}{4\mu}(a^2-\eta^2)W=\frac{1-\nu}{3}\frac{d^2}{4\mu h}(a^2-1)^{\frac{1}{2}}(a^2-\eta^2)^{\frac{1}{2}}P(a,\eta), \tag{3}$$

$$W=\frac{2}{\omega^2\rho d}\left(\frac{a^2-1}{a^2-\eta^2}\right)^{\frac{1}{2}}\frac{\partial P}{\partial\xi}(a,\eta), \tag{4}$$

$$\frac{\partial}{\partial\eta}\left[(1-\eta^2)\frac{\partial P}{\partial\eta}\right]+\frac{\partial}{\partial\xi}\left[(\xi^2-1)\frac{\partial P}{\partial\xi}\right]+\left(\frac{\omega d}{2c}\right)^2(\xi^2-\eta^2)P=0, \tag{5}$$

and

$$U(\pm1)=0, \tag{6}$$

where ν is Poisson's ratio, μ is the shear modulus, ρ_s is the mass density of the shell material, ρ is the density of the fluid, and c is the velocity of sound in the fluid. Equations 2 and 3 are the shell equations of motion, Eq. 5 is the fluid field equation, and Eq. 4 states that the normal shell velocity must be equal to that of the fluid on its surface. Except for a change of sign in Eq. 3, Eqs. 2–6 are identical to those for the shell surrounded by fluid.[7] Here, Eq. 5 must be satisfied in the region $1\leq\xi<a$, $-1\leq\eta\leq+1$.

By eliminating U and W from Eqs. 2–4, as outlined in Appendix A, a boundary condition on P only is

[1] H. Lamb, "On the Vibrations of a Spherical Shell," Proc. London Math. Soc. 14, 50–56 (1882).

[2] J. W. Strutt Lord Rayleigh, "On the Vibrations of a Gas Contained within a Rigid Spherical Envelope," Proc. London Math. Soc. 4, 93–103 (1872).

[3] P. J. Nemergut and R. S. Brand, "Axisymmetric Vibrations of Prolate Spheroidal Shells," J. Acoust. Soc. Am. **37**, 262–265 (1965).

[4] F. DiMaggio and R. Rand, "Axisymmetric Vibrations of Prolate Spheroidal Shells," J. Acoust. Soc. Am. 38, 179–186 (1966).

[5] P. M. Morse and H. Feshback, *Methods of Theoretical Physics* (McGraw-Hill Book Co., New York, 1953), Part II, pp. 1469–1472.

[6] C. Flammer, *Spheroidal Wave Functions* (Stanford University Press, Stanford, Calif., 1957).

[7] T. Yen and F. DiMaggio, "Forced Vibrations of Submerged Spheroidal Shells," J. Acoust. Soc. Am. 41, 618–626 (1967).

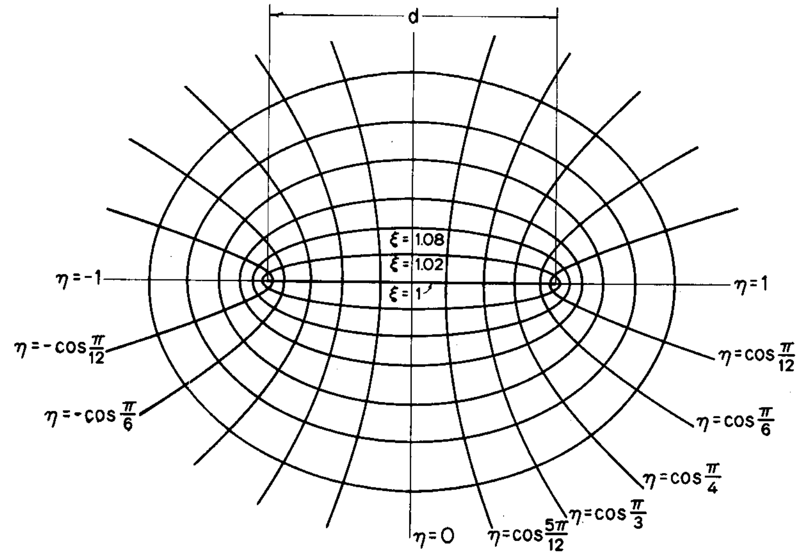

FIG. 1. Prolate spheroidal coordinate system.

obtained as

$$[h_1P_{\eta\eta\xi}+h_2P_{\eta\xi}+h_3P_{\xi}+h_4P_{\eta\eta}+h_5P_{\eta}+h_6P]=0,\quad \xi=a,\quad -1\leq\eta\leq 1 \tag{7}$$

where subscripts on P denote partial differentiation and the $h_i(\eta)$ are displayed in Appendix A.

It is seen from Appendix A and what follows that, for a given eccentricity and Poisson's ratio, natural frequencies will depend only on the parameters

$$\kappa=(\rho/\rho_s)(ad/2h) \tag{8}$$

and

$$\lambda=\rho_s c^2/2\mu=\tfrac{1}{2}(c/c_s)^2, \tag{9}$$

where

$$c_s=(\mu/\rho_s)^{\frac12} \tag{10}$$

is the velocity of propagation of shear waves in the shell material.

II. ELASTIC SPHERICAL SHELLS

Equations for a spherical shell of radius R may be obtained from Eqs. 2–7 by letting

$$d\rightarrow 0 \quad\text{and}\quad \xi\rightarrow\infty$$

such that

$$\xi d\rightarrow 2r \quad\text{and}\quad ad\rightarrow 2R \tag{11}$$

and

$$\eta=\cos\theta, \tag{12}$$

where r is the radial coordinate and θ the polar angle, as

$$-(1-\eta^2)^{\frac12}\frac{d^2}{d\eta^2}[(1-\eta^2)^{\frac12}U]-(1-\nu)U-(1-\eta^2)^{\frac12}(1+\nu)\frac{dW}{d\eta}-\frac{1-\nu}{2}\frac{\rho_sR^2\omega^2}{\mu}U=0, \tag{13}$$

$$(1+\nu)\frac{d}{d\eta}[(1-\eta^2)^{\frac12}U]+2(1+\nu)W-\frac{1-\nu}{2}\frac{\rho_sR^2\omega^2}{\mu}W=\frac{1-\nu}{2}\frac{R^2}{h\mu}P(R,\eta), \tag{14}$$

$$W=\frac{1}{\omega^2\rho}\frac{\partial P}{\partial r}(R,\eta), \tag{15}$$

$$\frac{\partial}{\partial\eta}\left[(1-\eta^2)\frac{\partial P}{\partial\eta}\right]+\frac{\partial}{\partial r}\left(r^2\frac{\partial P}{\partial r}\right)+\frac{\omega^2}{c^2}r^2P=0, \tag{16}$$

$$U(\pm1)=0, \tag{17}$$

and

$$[g_1P_{\eta\eta r}+g_2P_{\eta r}+g_3P_r+g_4P_{\eta\eta}+g_5P_{\eta}+g_6P]=0,\quad r=R, \tag{18}$$

where the $g_i(\eta)$ are displayed in Appendix A.

By separation of variables, bounded solutions to Eq. 16 for the pressure mode are obtained as

$$P(r,\eta)=r^{-\frac12}J_{n+\frac12}[(\omega/c)r]L_n(\eta), \tag{19}$$

where L_n is the Legendre polynomial of degree n and $J_{n+\frac12}$ is the Bessel function of order $n+\frac12$. Substituting Eq. 19 into Eq. 18, noting that

$$(1-\eta^2)L_n''-2\eta L_n'+n(n+1)L_n=0,$$

where primes denote differentiation with respect to η, and using[8]

$$dJ_{n+\frac12}(\alpha)/d\alpha=[(n+\tfrac12)/\alpha]J_{n+\frac12}(\alpha)-J_{n+\frac32}(\alpha),$$

[8] G. N. Watson, *Theory of Bessel Functions* (Cambridge University Press, Cambridge, England, 1923), p. 18.

the frequency equation for

$$z=\omega R/c \tag{20}$$

if obtained as

$$\left\{\left[\left(\frac{1-\nu}{1+\nu}\right)\lambda z^2-2\right](1+\lambda z^2)+n(n+1)\left(1-\frac{\lambda z^2}{1+\nu}\right)\right\}\left[n-z\frac{J_{n+\frac{3}{2}}(z)}{J_{n+\frac{1}{2}}(z)}\right]+\kappa_0\lambda z^2\left[\left(\frac{1-\nu}{1+\nu}\right)(1+\lambda z^2)-\frac{n(n+1)}{1+\nu}\right]=0, \tag{21}$$

whose solutions z for a given mode number n depend only on ν and the parameters λ and

$$\kappa_0=(\rho/\rho_s)R/h, \tag{22}$$

which is the spherical counterpart of the κ of Eq. 8 and can be obtained from it by performing the limiting operations of Eq. 11.

The corresponding displacement modes may now be found from Eqs. 13–15 as

$$W(\eta)=\frac{L_n(\eta)}{\omega^2\rho R^{\frac{3}{2}}}\left[nJ_{n+\frac{1}{2}}(z)-zJ_{n+\frac{3}{2}}(z)\right] \tag{23}$$

and

$$U(\eta)=\frac{(1-\eta^2)^{\frac{1}{2}}\frac{dL_n}{d\eta}}{\omega^2\rho R^{\frac{3}{2}}}\frac{1}{1+\lambda z^2}\left\{\left[n\left(1-\frac{\lambda z^2}{1+\nu}\right)-\frac{\lambda\kappa z^2}{1+\nu}\right]J_{n+\frac{1}{2}}(z)-z\left(1-\frac{\lambda z^2}{1+\nu}\right)J_{n+\frac{3}{2}}(z)\right\}. \tag{24}$$

From Eq. 22, it is seen that

$$\lim_{\substack{\rho\to 0\\ \rho_s\,\text{finite}}}\kappa_0=\lim_{\substack{\rho_s\to\infty\\ \rho\,\text{finite}}}\kappa_0=0. \tag{25}$$

Correspondingly, Eq. 21 is satisfied for $\kappa_0=0$ if either

$$\left[\left(\frac{1-\nu}{1+\nu}\right)\lambda z^2-2\right](1+\lambda z^2)+n(n+1)\left(1-\frac{\lambda z^2}{1+\nu}\right)=0, \tag{26}$$

which is Lamb's[1] frequency equation for a spherical shell *in vacuo*, or

$$n-z\left[J_{n+\frac{3}{2}}(z)/J_{n+\frac{1}{2}}(z)\right]=0, \tag{27}$$

which is a different form of the frequency equation for a fluid-filled rigid spherical shell obtained by Rayleigh.[2] For sufficiently small values of κ_0, the frequency spectrum corresponding to Eq. 21 should be well approximated by superposing the spectra for Eqs. 26 and 27.

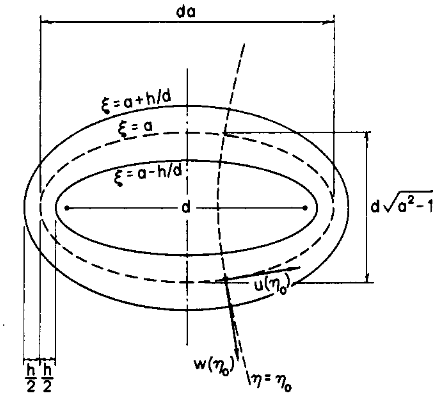

Fig. 2. Geometry of shell.

III. NUMERICAL RESULTS FOR SPHERICAL SHELLS

Figure 3 is a plot of the frequency spectrum for any fluid in a rigid spherical shell, obtained from Eq. 27. (It is to be noted that this and all other spectra plotted in this paper are discrete, i.e., only those points corresponding to integral values of the mode number n are physically meaningful.) Figure 4 is a similar plot for spherical shells *in vacuo* obtained from Eq. 26, using $c_s/c=2.205$ and $\nu=0.33$, which corresponds to an aluminum shell if c is the value for water. Superposition of the spectra of Figs. 3 and 4 yields Fig. 5, which should be a good approximation to the spectrum of Eq. 21 for small values of κ_0. For $\kappa_0=0.158$, e.g., the spectrum corresponding to Eq. 21 is indistinguishable from that of Fig. 5.

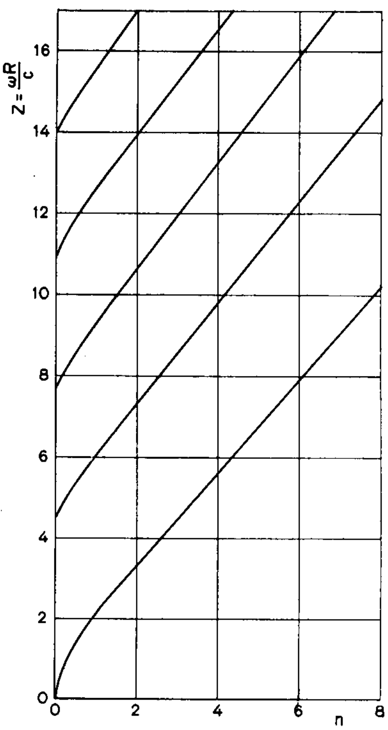

Fig. 3. Frequency spectrum for a rigid fluid-filled spherical shell.

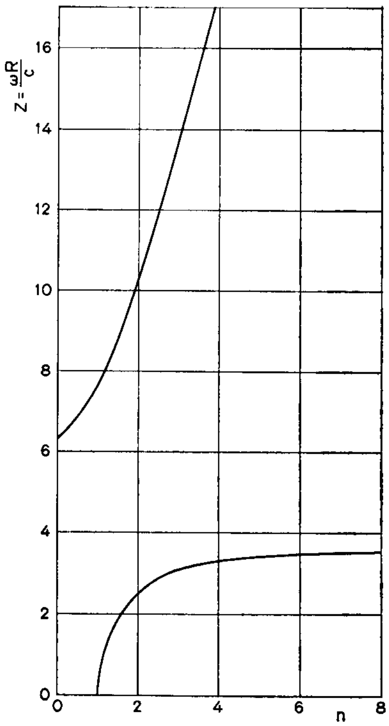

FIG. 4. Frequency spectrum for an elastic spherical shell *in vacuo* for $\nu=0.33$ and $c_s/c=2.205$.

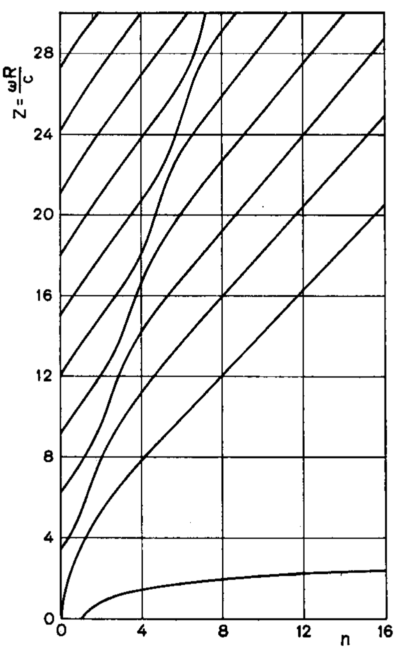

FIG. 6. Frequency spectrum for an elastic fluid-filled spherical shell for $\nu=0.33$, $\lambda=0.103$, $\kappa_0=17.60$.

In Fig. 6, the spectrum of Eq. 21 is plotted for

$$\nu=0.33,\quad c_s/c=2.205,\quad \rho_s/\rho=2.699,\quad h/R=0.02105,$$

which corresponds to an aluminum shell filled with water. For these values, Eqs. 9 and 22 yield

$$\lambda=0.103,\quad \kappa_0=17.60.$$

It is easily seen that Fig. 5 is no longer a good approximation of the spectrum for this value of κ_0 for a spherical shell. Figure 7 is a plot of the mode shape for $n=2$ obtained from Eqs. 23 and 24 for these same parameters.

In Fig. 8, the spectrum of Eq. 23 is plotted for

$$\nu=0.33,\quad \lambda=6.00,\quad \kappa_0=17.60.$$

For this value of λ, the upper branch of the spectrum of Eq. 26 is below the lowest branch of that of Eq. 27.

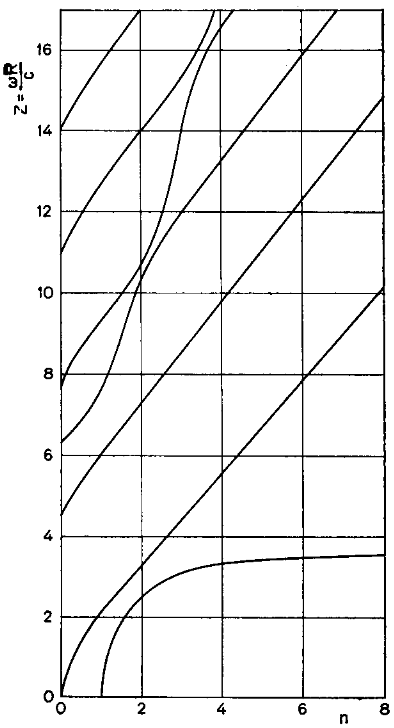

FIG. 5. Superposition of frequency spectra of Figs. 3 and 4.

IV. RIGID PROLATE SPHEROIDAL SHELLS

Setting the radial velocity of the shell equal to zero, Eq. 4 becomes

$$(\partial P/\partial\xi)(a,\eta)=0. \tag{28}$$

Bounded solutions of Eq. 5 are obtained using separation of variables as[6]

$$P(\xi,\eta)=R_{0n}^{(1)}(\gamma,\xi)S_{0n}(\gamma,\eta) \tag{29}$$

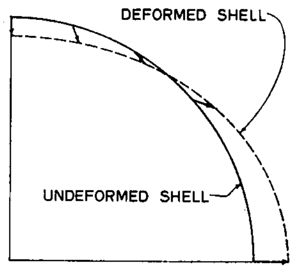

FIG. 7. Displacement mode for an elastic fluid-filled spherical shell for $\nu=0.33$, $\lambda=0.103$, $\kappa_0=17.60$, $n=2$, and $z=5.37$.

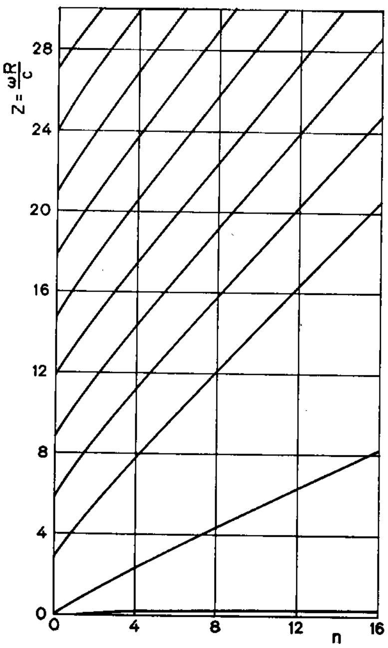

FIG. 8. Frequency spectrum for an elastic fluid-filled spherical shell for $\nu=0.33$, $\lambda=6.00$, $\kappa_0=17.60$.

where

$$\gamma=\omega d/2c \tag{30}$$

and $R_{0n}^{(1)}$ and S_{0n} are, respectively, the prolate spheroidal radial and angle functions of the first kind, order zero, and degree n. Substitution of Eq. 29 into Eq. 28 yields the frequency equation

$$dR_{0n}^{(1)}(a)/d\xi=0. \tag{31}$$

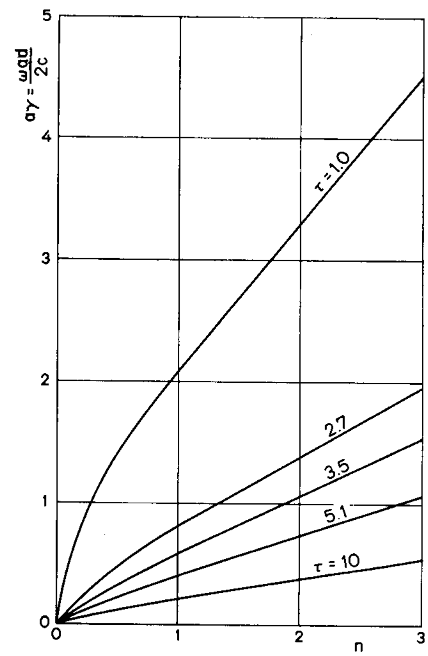

FIG. 9. Lowest branch of the frequency spectrum for rigid fluid-filled prolate spheroidal shells of various ratios of major to minor axis.

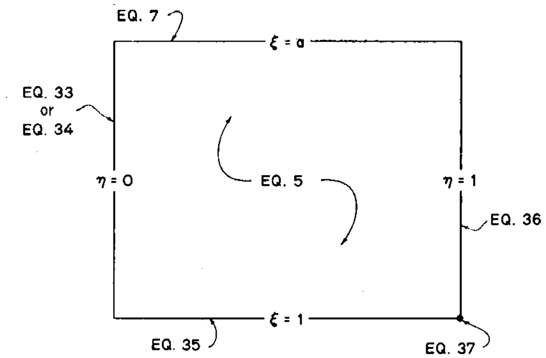

FIG. 10. Transformed domain and governing equations.

V. NUMERICAL RESULTS FOR RIGID PROLATE SPHEROIDAL SHELLS

Figure 9 is a plot of the lowest branches of the spectra of Eq. 31 for the first few modes of shells with various ratios of major to minor axis given by

$$\tau=a/(a^2-1)^{\frac{1}{2}}. \tag{32}$$

The plots for $\tau>1$ were obtained using all available tabulated values of $dR_{0n}^{(1)}/d\xi$ on pp. 168 and 169 of Ref. 6, while the curve for $\tau=1$, corresponding to a spherical shell, is identical to the lowest branch of Fig. 3.

VI. ELASTIC PROLATE SPHEROIDAL SHELLS

In Appendix B, it is shown that a single product of the form of Eq. 29, which represents bounded solutions to Eq. 5, cannot satisfy Eq. 7. A numerical method of solution has therefore been developed.

By considering separately symmetric modes (n even), for which

$$P(\xi,\eta)=P(\xi,-\eta), \tag{33}$$

and antisymmetric modes (n odd) for which

$$P(\xi,\eta)=-P(\xi,-\eta), \tag{34}$$

the original domain of integration is halved by making it unnecessary to consider negative values of η.

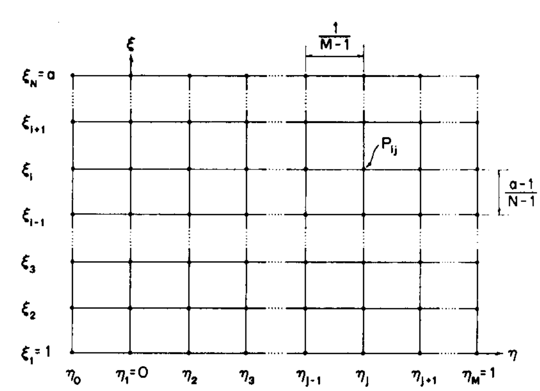

FIG. 11. Grid system used for numerical integration.

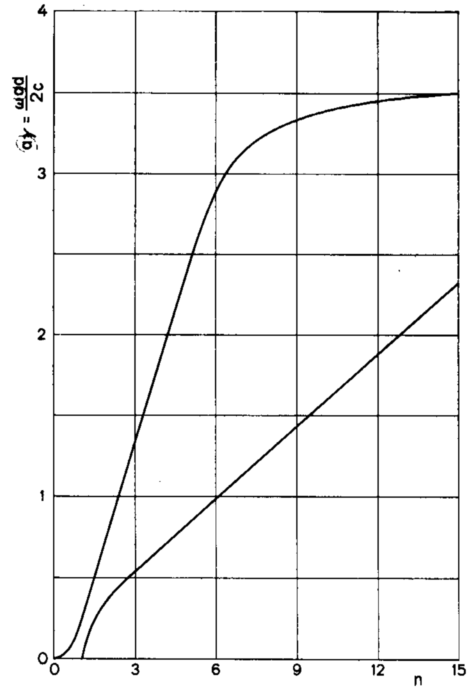

FIG. 12. Frequency spectrum for an elastic fluid-filled prolate spheroidal shell, for $\nu=0.33$, $\lambda=0.103$, $\kappa=17.60$, $\tau=10.0$.

For solutions with bounded second derivatives, Eq. 5 is replaced along the major axis of the shell by

$$\left[(1-\eta^2)\frac{\partial^2 P}{\partial\eta^2}-2\eta\frac{\partial P}{\partial\eta}+2\frac{\partial P}{\partial\xi}+\left(\frac{\omega d}{2c}\right)^2(1-\eta^2)P\right]=0,$$

$$\xi=1,\quad 0\leq\eta<1 \qquad (35)$$

$$\left[-2\frac{\partial P}{\partial\eta}+(\xi^2-1)\frac{\partial^2 P}{\partial\xi^2}+2\xi\frac{\partial P}{\partial\xi}+\left(\frac{\omega d}{2c}\right)^2(\xi^2-1)P\right]=0,$$

$$\eta=+1,\quad 1<\xi<a \qquad (36)$$

and

$$[\partial P/\partial\xi-\partial P/\partial\eta]_{\xi=1,\eta=1}=0. \qquad (37)$$

The problem consists of solving simultaneously Eq. 5 in the region $0\leq\eta<1$ and $1<\xi<a$, Eq. 35 at $\xi=1$ for $0\leq\eta<1$, Eq. 36 at $\eta=1$ for $1<\xi<a$, Eq. 37 at $\xi=1$, $\eta=1$ and Eq. 7 at $\xi=a$ and $0\leq\eta\leq1$, for modes satisfying Eq. 33 or Eq. 34. This is shown schematically in Fig. 10. Each of these equations was written in finite difference form with errors of second order in the spacing

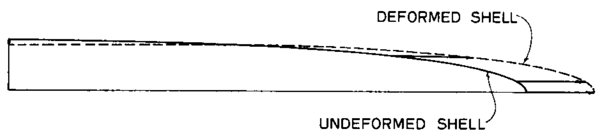

FIG. 13. Displacement mode for an elastic fluid-filled prolate spheroidal shell for $\nu=0.33$, $\lambda=0.103$, $\kappa=17.60$, $\tau=10.0$, $n=2$, and $a\gamma=0.7755$.

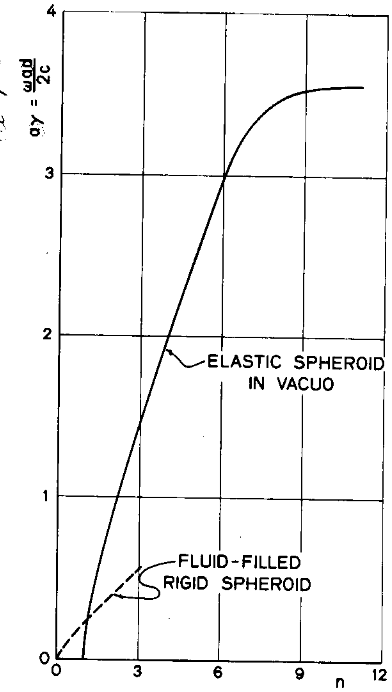

FIG. 14. Lowest branches of frequency spectra for an elastic spheroid *in vacuo* and a fluid-filled rigid spheroid, for $\tau=10.0$.

and applied to the $N(M+1)$ pivotal points shown in Fig. 11.

The resulting equations are of the form

$$\mathbf{AP}=0, \qquad (38)$$

where $\mathbf{A}$ is an $N(M+1)$ square matrix whose elements are functions of the frequency parameter γ of Eq. 30, and $\mathbf{P}$ is an $N(M+1)$ column matrix of the pressure mode elements P_{ij}. A trial-and-error process was used in which γ was assumed and det$\mathbf{A}$ calculated until

$$\det\mathbf{A}=0 \qquad (39)$$

was satisfied. For each value of γ satisfying Eq. 39, $\mathbf{P}$ was determined from Eqs. 38 and pivotal values of W and U from Eqs. 4 and A13.

By ordering Eqs. 38 with increasing η and ξ, $\mathbf{A}$ attains a maximum bandwidth of $4M+9$. Using the Gaussian-elimination–back-substitution technique (as incorporated in the LEQ[9] library routine) for $N(M+1)=150$, 30 sec was required on an IBM 7094 computer to evaluate det$\mathbf{A}$ for one assumed value of γ.

VII. NUMERICAL RESULTS FOR ELASTIC PROLATE SPHEROIDAL SHELLS

The numerical procedure outlined in Sec. VI was first checked by applying it to problems solved analytically in Secs. II–V. In particular, using $a=7(\tau=1.01)$, $\nu=0.33$, $\lambda=0.103$ and $\kappa=17.60$, results indistinguishable from those of Figs. 6 and 7 were obtained, while

[9] M. Goldstein, "Linear Equations Solution and Determinant Evaluation," SHARE Program No. SDA3239 (1964).

insertion of $a=1.005(\tau=10.0)$ and $a=1.077(\tau=2.69)$ for $\kappa=0$ produced results identical to those of Fig. 9 and Ref. 4.

In Fig. 12, the lowest two branches of the frequency spectrum for

$$a=1.005(\tau=10.0),\quad \nu=0.33,\quad \lambda=0.103,\quad \kappa=17.60$$

as obtained using the numerical method of Sec. VI are plotted. For the same parameters, Fig. 13 shows the mode shape for $n=2$ and $a\gamma=0.7755$.

It is of practical interest to note that, for this eccentricity, the spectra of Fig. 12 are excellently approximated by superposing the lowest branches of the spectra for an elastic shell *in vacuo* as obtained in Ref. 4 and for a rigid shell as plotted in Fig. 9. These are reproduced in Fig. 14. For this value of κ, this superposition was not valid for the spherical case, as demonstrated in Sec. III. It appears that as the eccentricity of the shell increases, the upper limit of κ for which this superposition is valid increases also.

ACKNOWLEDGMENT

This investigation was sponsored by the U. S. Office of Naval Research under contract with Columbia University.

Appendix A

To eliminate U and W from Eqs. 2–4, first multiply Eqs. 2 and 3 by $(a^2-\eta^2)^{3/2}$ and substitute the expression for W of Eq. (4) to obtain, at $\xi=a$,

$$f_1S''+f_2S+f_3P_{\eta\xi}+f_4P_{\xi}=Q=0 \tag{A1}$$

and

$$f_5S'+f_6S+f_7P_{\xi}+f_8P=T=0, \tag{A2}$$

where primes indicate differentiation with respect to η, subscripts ξ and η denote partial differentiation,

$$S=(1-\eta^2)^{1/2}(\omega^2\rho d/2a)U, \tag{A3}$$

$$f_1=(a^2-\eta^2)^{3/2}(1-\eta^2), \tag{A4}$$

$$f_2=(1-\nu)(a^2-\eta^2)^{3/2}[1+\lambda\gamma^2(a^2-\eta^2)], \tag{A5}$$

$$f_3=(1-\eta^2)[\nu(a^2-\eta^2)^2+(a^2-\eta^2)(a^2-1)], \tag{A6}$$

$$f_4=\eta(1-\eta^2)(4a^2-\eta^2-3), \tag{A7}$$

$$f_5=a^2(a^2-\eta^2)^{3/2}[\nu(a^2-\eta^2)/(a^2-1)+1], \tag{A8}$$

$$f_6=[1/(a^2-1)][-a^2(1-\nu)\eta(a^2-\eta^2)^{3/2}], \tag{A9}$$

$$f_7=a^2(a^2-\eta^2)^2/(a^2-1)+2\nu a^2(a^2-\eta^2)+a^2(a^2-1) -(1-\nu)(a^2-\eta^2)^3\lambda\gamma^2, \tag{A10}$$

and

$$f_8=(1/a)[-(1-\nu)\gamma^2\lambda\kappa(a^2-\eta^2)^3]. \tag{A11}$$

Now, referring to Eqs. A1 and A2 and noting that

$$f_1(f_5'+f_6)T+f_5^2Q-F_1f_5T_{\eta}=0, \tag{A12}$$

S is obtained in terms of P as

$$S=(1/s_5)(s_1P_{\eta\xi}+s_2P_{\eta}+s_3P+s_4P_{\xi}), \tag{A13}$$

where

$$s_1=f_5(f_1f_7-f_3f_5), \tag{A14}$$

$$s_2=f_1f_5f_8, \tag{A15}$$

$$s_3=f_1f_5f_8'-f_1f_8(f_6+f_5'), \tag{A16}$$

$$s_4=f_5(f_1f_7'-f_4f_5)-f_1f_7(f_5'+f_6), \tag{A17}$$

and

$$s_5=f_1f_6(f_5'+f_6)+f_5(f_2f_5-f_1f_6'). \tag{A18}$$

Finally, substituting Eq. A13 into Eq. A2, Eq. 7 is obtained with

$$h_1=f_5s_1s_5, \tag{A19}$$

$$h_2=f_5s_5s_1'+f_5s_4s_5-f_5s_1s_5'+f_6s_1s_5, \tag{A20}$$

$$h_3=f_5s_5s_4'-f_5s_4s_5'+f_6s_4s_5+f_7s_5^2, \tag{A21}$$

$$h_4=f_5s_2s_5, \tag{A22}$$

$$h_5=f_5s_5s_2'+f_5s_3s_5-f_5s_2s_5'+f_6s_2s_5, \tag{A23}$$

and

$$h_6=f_5s_5s_3'-f_5s_3s_5'+f_6s_3s_5+f_8s_5^2. \tag{A24}$$

The corresponding coefficients of Eq. 18 are obtained by performing analogous operations on Eqs. 13–15, as

$$g_1=(1-\eta^2)[1-\lambda z^2/(1+\nu)], \tag{A25}$$

$$g_2=-2\eta[1-\lambda z^2/(1+\nu)], \tag{A26}$$

$$g_3=(1+\lambda z^2)\{2-[(1-\nu)/(1+\nu)]\lambda z^2\}, \tag{A27}$$

$$g_4=-(1-\eta^2)\lambda\kappa_0z^2/(1+\nu)R, \tag{A28}$$

$$g_5=2\eta(\lambda\kappa_0z^2)/(1+\nu)R, \tag{A29}$$

$$g_6=-(1-\nu)(1+\lambda z^2)[\lambda\kappa_0z^2/R(1+\nu)]. \tag{A30}$$

Appendix B

If a solution of the form of Eq. 29 is to satisfy Eq. 7, then

$$[G'(\beta_1F'+\beta_2F)+G(\beta_3F'+\beta_4F)]=0,\quad \xi=a \tag{B1}$$

where

$$F(\xi)=R_{0n}^{(1)}(\gamma,\xi), \tag{B2}$$

$$G(\eta)=S_{0n}(\gamma,\eta), \tag{B3}$$

$$\beta_1=h_1\alpha_1+h_2\alpha_3, \tag{B4}$$

$$\beta_2=h_4\alpha_1+h_5\alpha_3, \tag{B5}$$

$$\beta_3=h_1\alpha_2+h_3\alpha_3, \tag{B6}$$

$$\beta_4 = h_4\alpha_2 + h_6\alpha_3, \qquad \text{(B7)}$$

$$\alpha_1 = -2\eta, \qquad \text{(B8)}$$

$$\alpha_2 = \lambda_{0n} - \gamma^2\eta^2, \qquad \text{(B9)}$$

$$\alpha_3 = -(1-\eta^2); \qquad \text{(B10)}$$

primes denote differentiation with respect to ξ or η, as appropriate; and use has been made of the equation defining S_{0n}, i.e.,[6]

$$(1-\eta^2)S_{0n}'' - 2\eta S_{0n}' + (\lambda_{0n} - \gamma^2\eta^2)S_{0n} = 0, \qquad \text{(B11)}$$

in which the $\lambda_{0n}(\gamma)$ are the prolate spheroidal eigenvalues of order 0 and degree n.

Equation B1 can be satisfied identically with respect to η (for $-1 \leq \eta \leq 1$) if and only if it is separable, i.e., if it can be written in the form

$$[a_0(\eta)G(\eta) + a_1(\eta)G'(\eta)][b_0F(a) + b_1F'(a)] \equiv 0, \qquad \text{(B12)}$$

in which case the frequency equation would be obtained by requiring the second bracket to vanish. Equation B1 can be put in the form of Eq. B12 if and only if the identities

$$b_0a_0(\eta) \equiv \beta_4(\eta), \qquad \text{(B13)}$$

$$b_0a_1(\eta) \equiv \beta_2(\eta), \qquad \text{(B14)}$$

$$b_1a_0(\eta) \equiv \beta_3(\eta), \qquad \text{(B15)}$$

and

$$b_1a_1(\eta) \equiv \beta_1(\eta) \qquad \text{(B16)}$$

are satisfied. But Eqs. B13 and B16 can be satisfied if and only if

$$\beta_1(\eta)\beta_4(\eta) - \beta_2(\eta)\beta_3(\eta) \equiv 0. \qquad \text{(B17)}$$

The identity of Eq. B17 is not satisfied by the $\beta_i(\eta)$ of Eqs. B13–B16. Therefore, a single product of the form of Eq. 29 cannot satisfy Eq. 7.